Induction Machine Stator Fault Tracking using the Growing Curvilinear Component Analysis

IEEE Access
Multidisciplinary ⋮ Rapid Review ⋮ Open Access Journal

Received November 11, 2020, accepted November 26, 2020, date of publication December 24, 2020,
date of current version January 6, 2021.

Digital Object Identifier 10.1109/ACCESS.2020.3047202

Induction Machine Stator Fault Tracking Using the Growing Curvilinear Component Analysis

RAHUL R KUMAR[1,3], (Student Member, IEEE), VINCENZO RANDAZZO[2], (Student Member, IEEE), GIANSALVO CIRRINCIONE[3,4,5], (Senior Member, IEEE), MAURIZIO CIRRINCIONE[3], (Senior Member, IEEE), EROS PASERO[2], (Member, IEEE), ANDREA TORTELLA[1], (Member, IEEE), AND MAURO ANDRIOLLO[1], (Member, IEEE)

[1]Department of Industrial Engineering, University of Padova, 35131 Padova, Italy
[2]Department of Electronics and Telecommunications, Politecnico di Torino, 10129 Turin, Italy
[3]School of Engineering and Physics, The University of the South Pacific, Suva, Fiji
[4]University of Picardie Jules Verne, 80000 Amiens, France
[5]Innovatives Technologies Laboratory (LTI), University of Picardie Jules Verne, 80000 Amiens, France

Corresponding author: Rahul R Kumar (rahulranjeev.kumar@studenti.unipd.it)

ABSTRACT Detection of stator-based faults in Induction Machines (IMs) can be carried out in numerous ways. In particular, the shorted turns in stator windings of IM are among the most common faults in the industry. As a matter of fact, most IMs come with pre-installed current sensors for the purpose of control and protection. At this aim, using only the stator current for fault detection has become a recent trend nowadays as it is much cheaper than installing additional sensors. The three-phase stator current signatures have been used in this study to observe the effect of stator inter-turn fault with respect to the healthy condition of the IM. The pre-processing of the healthy and faulty current signatures has been done via the in-built DSP module of dSPACE after which, these current signatures are passed into the MATLAB® software for further analysis using AI techniques. The authors present a Growing Curvilinear Component Analysis (GCCA) neural network that is capable of detecting and follow the evolution of the stator fault using the stator current signature, making online fault detection possible. For this purpose, a topological manifold analysis is carried out to study the fault evolution, which is a fundamental step for calibrating the GCCA neural network. The effectiveness of the proposed method has been verified experimentally.

INDEX TERMS Data streaming analysis, growing curvilinear component analysis, induction machine, neural networks, on-line fault diagnosis, principal component analysis.

I. INTRODUCTION

Research in the arena of Fault Diagnosis (FD) and Condition Monitoring (CM) of electrical machines has become a hot topic in this information age. This is due to rise in technological advancements and its involvement in an endless number of industrial applications. From the engineering point of view, concepts of FD and CM have always been the key issue to date. This is because maintaining assets when it comes to large motors or generators, are essential as failure of these types of motors may result in serious consequences and loss of money.

A reliable diagnostic system should exhibit an early identification of the incipient fault, thus resulting in a quick maintenance, ensuing a short downtime for the processes under consideration. For the aforesaid properties, it is important that the system is able to acquire adequate amount of data and extract useful information to correctly detect and classify the anomalies for the ongoing process. Additionally, the system should be able to recognize the normal operation under varying conditions. In the recent decade, there has been flourishing literature that involves development of the diagnostic schemes for electrical machines and drives to overcome the shortcomings instigated by the conventional methods.

Based on the statistics from authors of [1]–[3], the number of working machines across the world was approximated to be more than 16.1 billion in 2011, with a rapid increase of up

The associate editor coordinating the review of this manuscript and approving it for publication was Pinjia Zhang.

to 50% in the preceding five years. The most common ones are said to be the Induction Machines (IMs) that are widely used in industries due to its reliability and, compatibility with available power supplies. In addition to that, the IMs can also be integrated well when it comes to flywheels energy storage systems (FESS) [4]. While they are much more robust compared to other types of motors, they are liable to various sorts of faults like: mechanical, electrical and outer motor drive faults. A very prominent property of the IMs is that they are highly symmetrical systems. Therefore, any occurrence of fault may cause changes in its symmetrical properties, which would affect the whole operation of the motor under consideration.

Studies from the statistics available from IEEE and EPRI for motor faults [5]–[7] reveals that majority of faults arise from IMs as they contribute up to 80% of the failed components. On the other hand, according to the authors of [5]–[12], it is apparent that up to 30% of the causes in motor failures are due to stator based faults.

The stator fault begins as the inter-turn short circuit, after which, it evolves over time resulting in short circuit between the coils or the phase windings. This evolution of stator based fault may result in other faults that are mechanically and electrically related [13]. Hence, due to its catastrophic effects, it is essential to carry out diagnostics in real time in order to track the evolution of the fault [14], [15].

A very common way of analyzing the condition of a rotating machine is to make use of the motor current signature analysis (MCSA). The MCSA is straightforward and powerful under appropriate working conditions. Nonetheless, even if MCSA is the ideal method for electrical machines under steady state conditions and rated load, it is still not suitable to handle either IMs with special magnetic structure or IM operation in transient conditions, where alternative methodologies have been proposed in [16]–[20].

For the purpose of fault classification and decision making once the feature-set has been developed, AI based techniques are very instrumental [21], [22]. Generally, prior to classification stage, the type of features used is of utmost importance. A good feature set should be able demonstrate high variability and totality of the main [13], [23], [24]. This enables better training of classifiers and helps in ruling out the true negatives and false negatives. In literature, many feature selection and dimensionality reduction techniques demonstrate its capability in extracting noteworthy features to be ready from the raw/standardized dataset for faster processing when it comes to training the classifiers [25], [26]. The classification is normally done in either supervised or non-supervised fashion: under supervised learning, the classes are labelled whereas they are unknown under unsupervised learning. At the last stage of classification, final decision is made by the expert systems by utilizing the developed online framework of information bases.

For the purpose of online data processing and real time Dimensionality Reduction (DR), it is mandatory to acquire a continuous stream of input data. Under this scenario, the data is supposed to be extracted from a distribution which is stationary. In terms of the DR based techniques, it is apparent that linear methods perform faster DR and commonly use the Principal Component Analysis (PCA) as the base method. Stemming from this approach, the linear neural based techniques: Generalized Hebbian Algorithm (GHA [27] and the incremental PCA (candid covariance-free CCIPCA [28]) have been utilized. On the other hand, the non-linear DR techniques, though being accurate, are very time consuming and are not suitable for online applications. Over the years, numerous efforts have been made to reduce the time complexity of the non-linear DR techniques. Some of these approaches include: updating of the structure information (graph), new data prediction and embedding updating. The incremental variants (e.g. iterative Locally Linear Embedding (LLE) algorithm [29]) still appear to be computationally expensive and time consuming.

Furthermore, neural networks can also be exploited to project data or reduce their dimensionality. They are first trained in an offline way and, then, during the recall phase, work in real time. In general, they can be used only for stationary data; in this sense, these techniques can derive from the embedding its implicit model. Some instances would include self-organizing maps (SOM) [30] and their variants [31], [32].

In case of a stream of non-stationary data, such as those generated for fault and pre-fault diagnosis and modelling, the online Curvilinear Component Analysis (onCCA) and the growing Curvilinear Component Analysis (GCCA) have been proposed in [33]–[36]. These two methods exploit incremental quantization to track the non-stationarity; indeed, data clustering is performed together with a fast projection technique based on the Curvilinear Component Analysis (CCA [37], [38]).

In this paper, a method for online FD has been proposed. The technique is a growing variant of the CCA neural network that is capable of detecting non-stationarity in the data flow. In particular, the GCCA neural network is capable of detecting and follow the evolution of a phase fault in an IM. The proposed technique only utilizes the stator current spectrum of the IM and performs FD by observing changes in the data distribution in a three dimensional map. Using the idea of ''bridges'', the GCCA correctly detects the non-stationarity (the faulty scenarios) by examining the bridges when the data stream transitions from healthy to faulty region. It must be noted that this FD procedure has been applied to FESS, where early detection of faulty conditions of the driving IM is important for safety and maintenance reasons.

This paper is organized as follows: In Section II, the method of GCCA is explained in detail, after which, the explanation about the experimental setup is given in Section III, Part A. In Part B of Section III, details on stator fault experimentation and some preliminary results involving Space Vector loci are presented together with comments. Thereafter, the results with detailed explanations involving

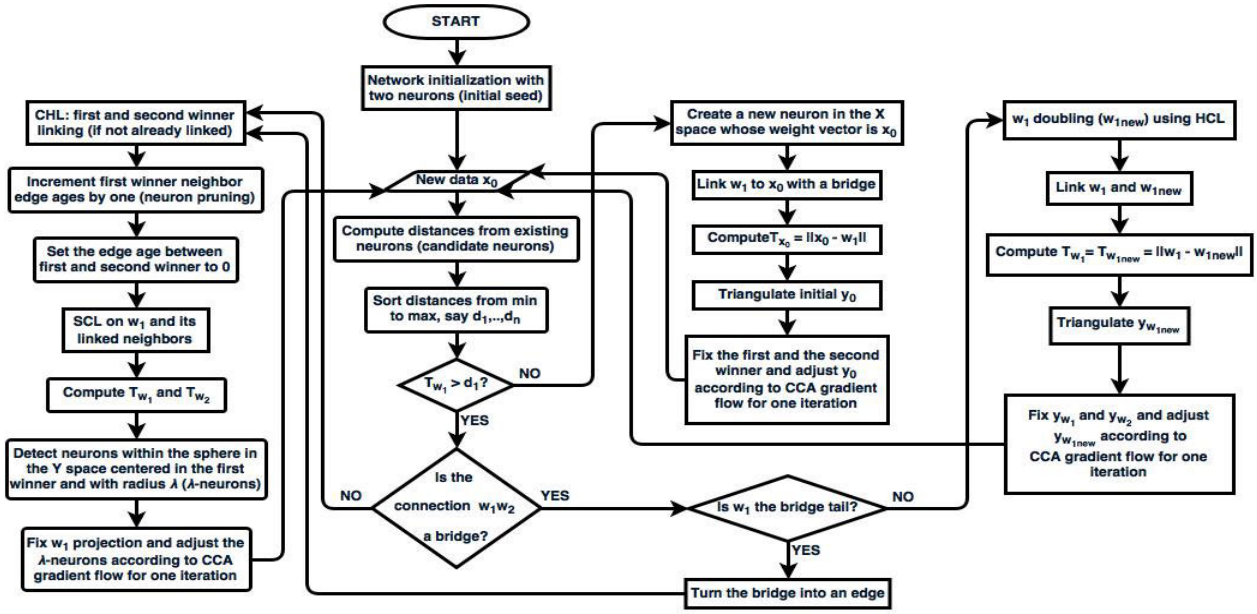

FIGURE 1. GCCA flowchart.

GCCA are presented in Section IV. The concluding remarks are summarized in Section V of the paper.

II. THE GROWING CURVILINEAR COMPONENT ANALYSIS

The Growing Curvilinear Component Analysis (GCCA) is an incremental neural network, it is self-organized and it has been designed to deal with non-stationarity. To handle such complexity, two mechanisms have been implemented: ''seeds'' and ''bridges''. The former are pairs of neurons used to explore a new region of the input domain; the latter are special kind of links that track the non-stationarity in the input (i.e. the fault indicator in this case). Indeed, GCCA exploits bridges and seeds to learn how the input evolves over time. Fig. 1 shows the training algorithm flowchart [39].

GCCA is both supervised and incremental. Its number of neurons is determined automatically by the input space quantization. Each neuron has two weight vectors: one in the input space (X-weight) and one in the output space (Y-weight), which gives the data projection. To better approximate the input data distribution, each neuron is equipped with a threshold. This threshold represents its Voronoi region in the input space. The previously mentioned threshold is local, i.e. neuron specific and is used to ascertain the novelty of the input data with respect to the existing quantization. It is automatically computed as the distance in the X-space between the neuron and its farthest neighbor (according to the network topology). If the input data is novel with respect to the X-space closest-neuron (i.e. the first-winner) threshold, a new neuron is created whose weight vector in the X-space is the data itself; in the Y-space, the weight, i.e. the data projection, is determined as in CCA. On the contrary, if the data fails the novelty test, the first-winner and its neighbors adapt their weight vectors in the X space by means of the Soft Competitive Learning (SCL [33, 34]); as in the previous case, their projections are updated as in CCA.

To differentiate between stationarity and non-stationarity, GCCA neurons can be connected using two kind of links: edges, which determine the data manifold topology according to the Competitive Hebbian Learning (CHL [40]), or bridges, which track a change in the input distribution (e.g. a jump).

A bridge is a special kind of directional connection created to link a new neuron to the previous quantization, i.e. the network; it points towards the new neuron, which, as explained above, represents a change, i.e. a non-stationarity, in the input data.

A seed is a couple of neurons made of a neuron and its double, whose weight vector is given by the hard competitive learning, HCL [33], [34]. Neuron-doubling is done every time the first-winner is the top of a bridge departing from the second-close neuron (i.e. the second-winner); in this sense, this technique populates a novel part of the input manifold. Conversely, if the first-winner is the bridge tail, the region previously linked with a bridge does not correspond to non-stationarity (e.g. a jump) in the input distribution; as a consequence, that connection is turned into an edge which, as described above, conveys information about the manifold topology (i.e. stationarity).

It is worth mentioning that GCCA is incremental and adaptive, i.e. it changes the amount of connections and neurons over time by creating them as explained above or, pruning by age algorithm.

The projection is based on CCA, which exploits a distance-preserving technique, to preserve distances smaller than λ in the output space.

III. METHODOLOGY

A. EXPERIMENTAL TEST RIG

To develop the database, an experimental setup has been constructed. The setup includes a three-phase squirrel cage IM of 1.1 kW rating that is connected to a SEMIKRON IGBT Voltage Source Inverter (VSI) which is of 12 kVA. The parameters of the IM used is described in Table 3. For acquisition of current signals, the LEM (LA 55-P) current transducers have been used in conjunction with DS1104 card (dSPACE). The data was acquired at a sampling frequency of 10 kHz. Fig. 2 shows the experimental setup used in this study.

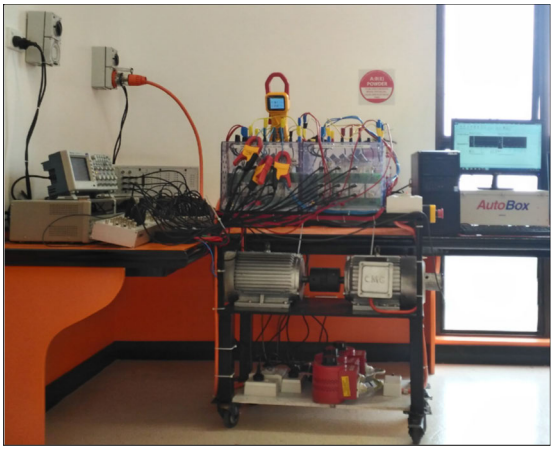

FIGURE 2. Experimental test rig.

B. STATOR FAULT EXPERIMENTATION: DATA ACQUISITION AND DESCRIPTION

In order to develop a database, the three-phase stator current signals were acquired from two identical IMs (parameters listed in Table 1) with similar manufacturing conditions. For both the IMs, data was acquired for inverter fed condition via scalar control method [41]. For both the cases (healthy and faulty), data was acquired for 0%, 25% and 40% loading conditions (full load torque is 7 Nm).

TABLE 1. Induction motor parameters.

Parameter	Value
No. poles	4
Supply Frequency	50 Hz
Stator Resistance	3.6760 Ω
Rotor Resistance	3.8270 Ω
Stator Leakage Inductance	0.0268 H
Rotor Leakage Inductance	0.0400 H
Magnetizing Inductance	0.4490 H
Moment of Inertia	0.0025 kgm^{-2}

The inter-turn short circuit has been introduced in one of the coils of Phase C as shown in Fig. 3. To quantify the percentage of inter-turn short circuit (ITSC) in a phase,

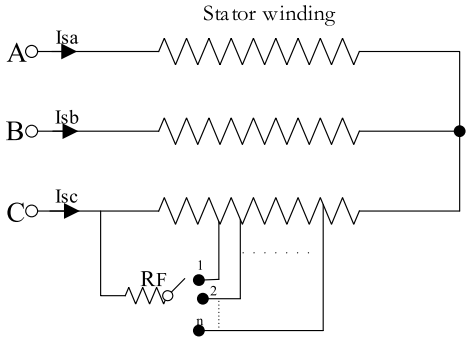

FIGURE 3. Schematic for stator fault.

the following calculation using the resistance quantities in % has been used (1):

$$\%ITSC = \frac{R_{no.windings\ shorted}}{R_{totalno.windings\ inaphase}} \times 100 \tag{1}$$

The level of fault (% ITSC) ranges from 0% to 10%, according to the connected shunt resistor R_F. This shunt resistor R_F has been used to restrict the circulating currents in the shorted portion of the stator winding under each level of fault severity. This is done to ensure a safe level of circulating current to avoid permanent damage to the motor windings.

For no load condition, the level of fault severity goes up to 10.92%, while for the other two loading conditions, it goes from healthy (0%) to 6.85% of the inter-turn short circuit in the stator winding. It has been noted for the faulty case that as the level of severity increases due to stator inter-turn fault, higher vibration and temperature is observed on the motor under test.

In Figs. 4-6, the time evolution of the faulty current signature with respect to the healthy condition of IM has been shown. While visualizing the time domain stator current signatures (Figs. 4-5) is not enough to deduce the condition of the IM, the corresponding Space Vector Loci (SVL) has been used. In Fig. 6, the load variation of a healthy IM from 0%

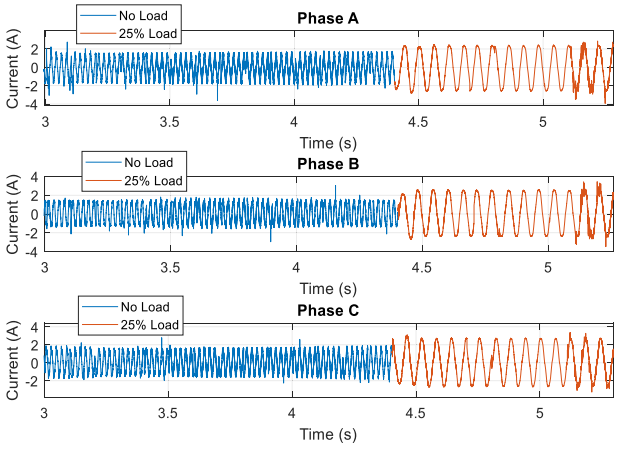

FIGURE 4. Three phase current - healthy motor.

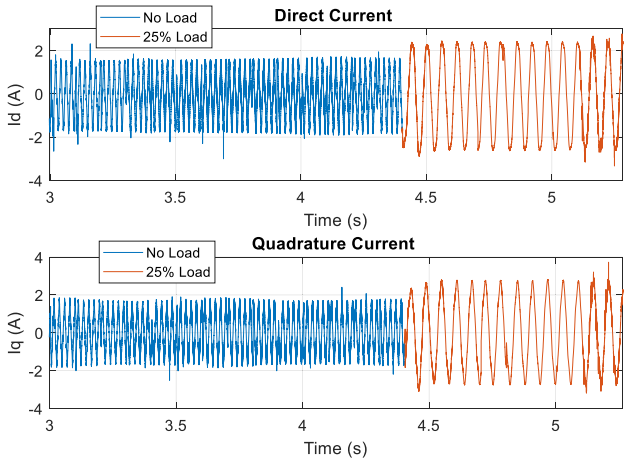

FIGURE 5. Space vector current - healthy motor.

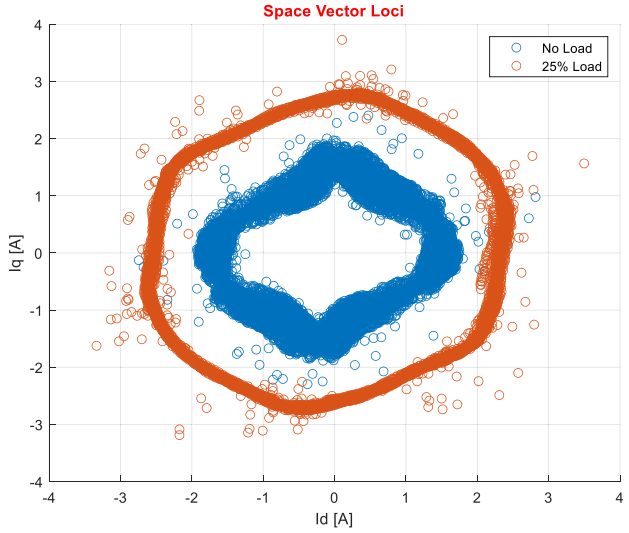

FIGURE 6. SVL - healthy motor.

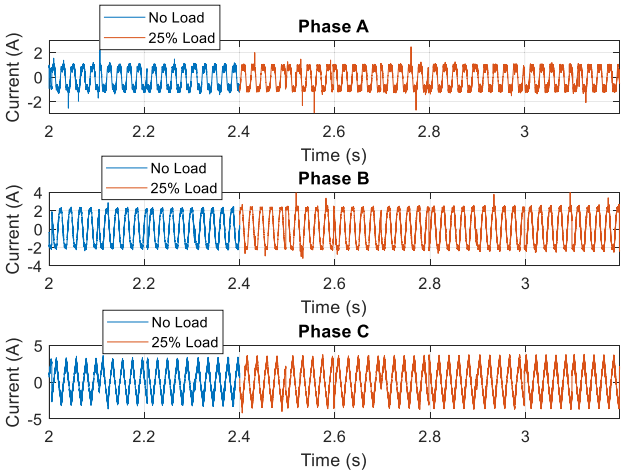

FIGURE 7. Three phase current - faulty motor.

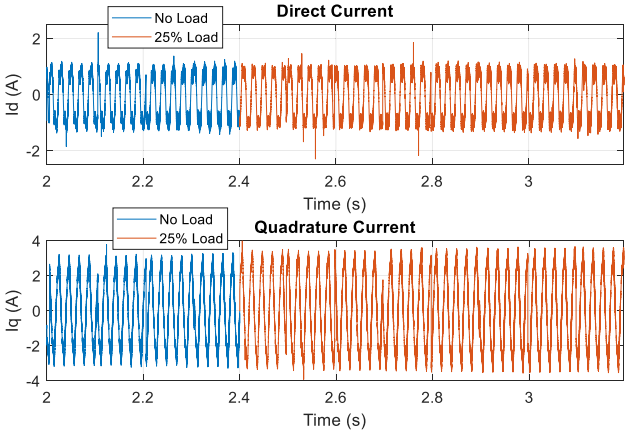

FIGURE 8. Space vector current - faulty motor.

to 25% at time instant of 4.4s is apparent. Under these circumstances, all the phases in IM appear to be balanced and any rise in amplitude is proportional to the change in the SVL radius. To highlight these changes, the inner hexagonal like figure in Fig. 6 corresponds to the healthy IM operating at 0% load ($t = 3.0s$ to $t = 4.4s$). On the other hand, from $t = 4.4s$ onwards, due to load change (from 0% to 25%), similar hexagonal pattern is maintained except it expands and becomes larger. It must be noted that the hexagonal pattern is due to harmonics induced by the VSI.

Similar remarks can be made for the faulty case where Figs. 7-8 represent the phase and space vector currents, respectively. The fault is introduced in phase C and its severity is about 5%. While a sudden jump may not be very noticeable, but considering the reading on the y-axes of Figs. 7-8, there is a significant rise in the amplitude of the phase and space vector currents compared to the healthy scenario. The corresponding SVL for the faulty case (Fig. 9) however, is in form of a hysteresis pattern and inflates upon increasing the load from 0% ($t = 2.0s$ to $t = 2.4s$) to 25% at time instant of 2.4$s$and onwards.

Under faulty scenario, in order to track the severity of fault, Figs. 10-12 represent the evolution of fault under 0%, 25% and 40% loading conditions. The levels of fault (percentage of fault) are varied in Phase C of the IM by switching to the loops corresponding to different number of windings in a coil (see Fig. 3). In case of no-load condition, the stator inter-turn fault ranged up to 10.92%, whereas for 25% and 40% loading condition, the fault severity went up to 6.85%. The transition between transient and steady state conditions are also observed in the space-vector maps. In particular, as the fault severity increases, the patterns in SVL in Figs. 10-12 changes to a hysteresis like figure and, for each level of fault, the shape becomes larger.

It should be noted that the space vector maps show the fault patterns with varying load conditions as well as different fault severities. In the following section, the GCCA will be utilized to obtain the same fault patterns (as in Figs. 10-12).

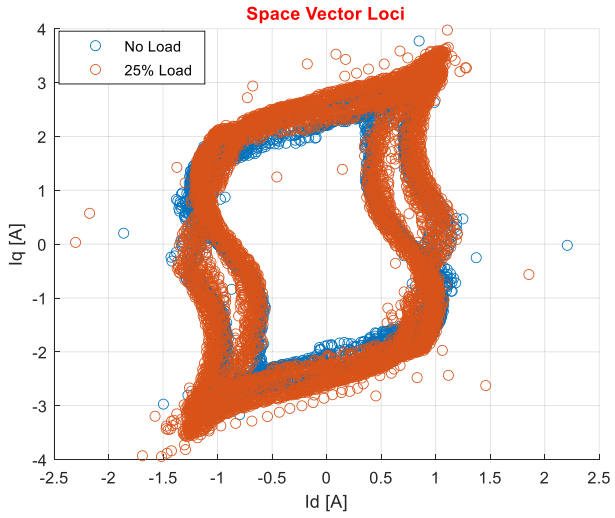

FIGURE 9. SVL - Faulty Motor.

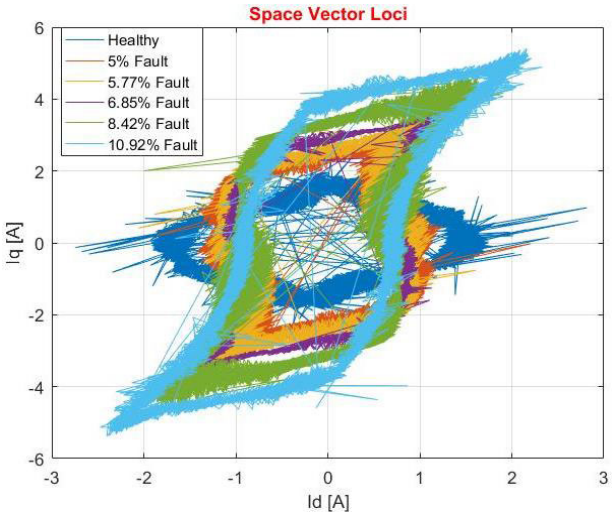

FIGURE 10. Stator inter-turn short circuit SVL – no load.

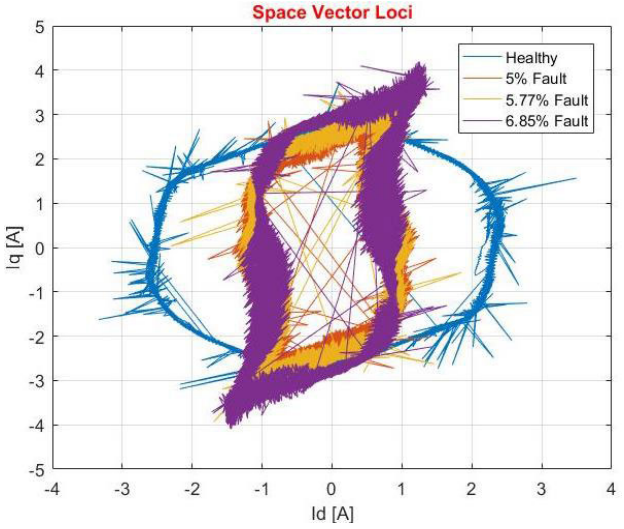

FIGURE 11. Stator inter-turn short circuit SVL – 25% load.

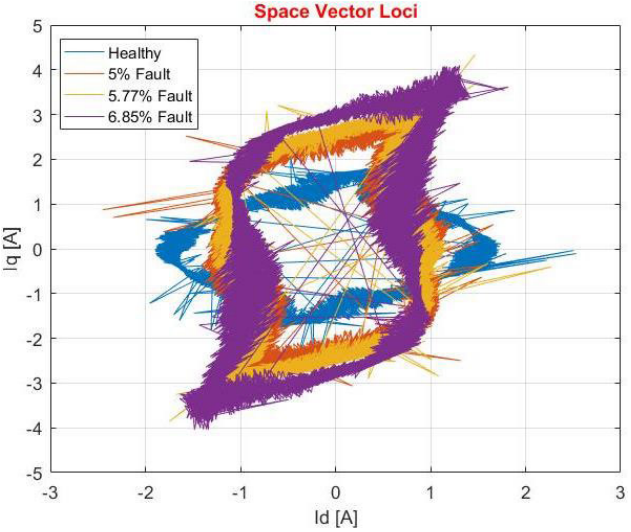

FIGURE 12. Stator inter-turn short circuit SVL – 40% load.

The reduction of the dimension of the original data space (created by considering the three phase currents) to 2 dimensions will indicate the inception of the fault using the idea of bridges.

IV. EXPERIMENTATION USING GROWING CCA

A. STATOR FAULT EXPERIMENT: DIMENSIONALITY REDUCTION AND FAULT DETECTION USING THREE PHASE CURRENT

The experiments described above have been further investigated using GCCA. The prime focus at this aim is to: (a) demonstrate GCCA's ability upon reducing the dimension from 3 (three-phase currents) to 2. A notable fact here is that unlike space vectors (which is just a fixed transformation of 3-phase currents to 2), GCCA is adaptive and can be applied to various dimensions. Results in Figs. 13-15 coincide approximately with the patterns observed in Figs. 10-12. (b) indicate the evolution of the fault (though rapid) via bridges (fault detection).

The network has only been trained with the 3-phase current data with parameters listed in Table 2. It follows the input evolution over time and, simultaneously, projects it in the latent current space in real time.

Fig. 13 shows the input quantization by means of the X-neurons together with their connections (edges are blue, bridges are red), in case of machine with no load. The quantization is very accurate; although the fault evolution is very rapid, all the different time intervals are represented properly. Furthermore, non-stationarity of the current is learned by the presence of bridges and their density. Some outliers are present because, currently, no technique to handle these cases has been adopted; however, if needed, it is simple to provide the network with an outlier detection method to increase its robustness.

TABLE 2. GCCA parameters.

Parameter	Value
α	0.05
λ	0.30
α_1	0.40
α_n	0.04
age_{max}	4
Epochs	5

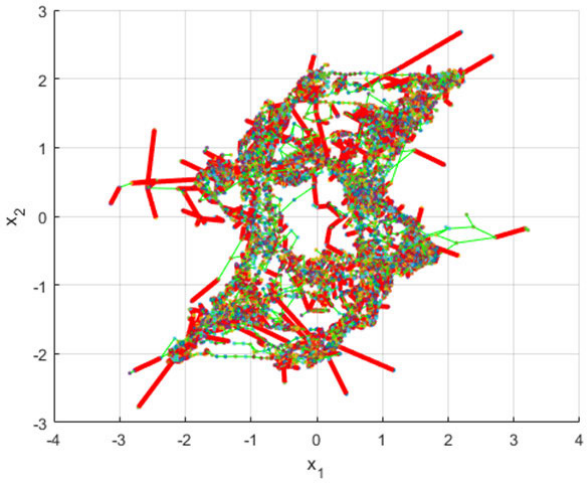

FIGURE 13. Input neurons with connections under no load conditions.

The GCCA quantization together with its projection can be exploited in many ways: for instance, an increasing number of bridges indicates the onset of a pre-fault condition in the machine: actually, Fig. 13 shows both GCCA output as well as the overall quantization of the input space.

As more damage occurs in the IM, more and more bridges appears to record the changes, i.e. the non-stationarity, in the stator current. This is clearly shown by the change of the hysteresis like pattern, as the fault level increase. Fig. 13 also demonstrates how different can be non-stationarities; indeed, the shape of the healthy and faulty are well distinguishable. Albeit bridges appearance depicts the onset of the fault, they will also be created in a similar way even if the time change is sudden; at this purpose, the turn-into-edge technique has been introduced to mitigate this kind of situations.

Different from other neural architectures, which generally require constant parameters to deal with non-stationarity, GCCA does not only detect the pre-fault condition, but also records the whole evolution of the machine.

The same considerations hold for a machine with, respectively, 25% (Fig. 14) and 40% (Fig. 15) load. The healthy and faulty trajectories are very well separated, thus allowing all the faults to be recognized.

B. STATOR FAULT EXPERIMENT: FEATURE CALCULATION AND MANIFOLD ANALYSIS

As the stator inter-turn fault is an evolving fault in nature, stationary techniques fail to detect this type of fault and

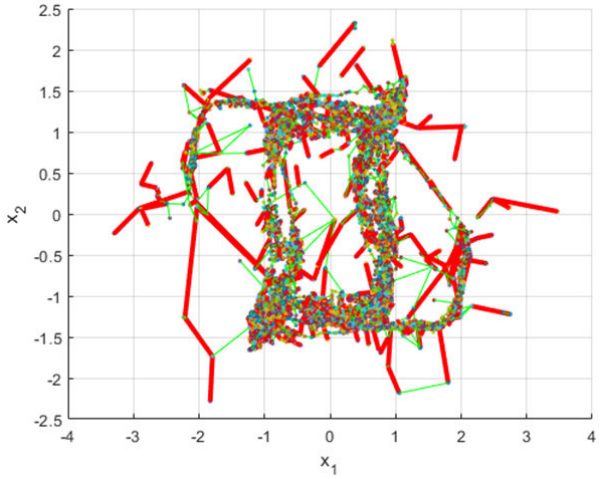

FIGURE 14. Input neurons with connections under 25% load conditions.

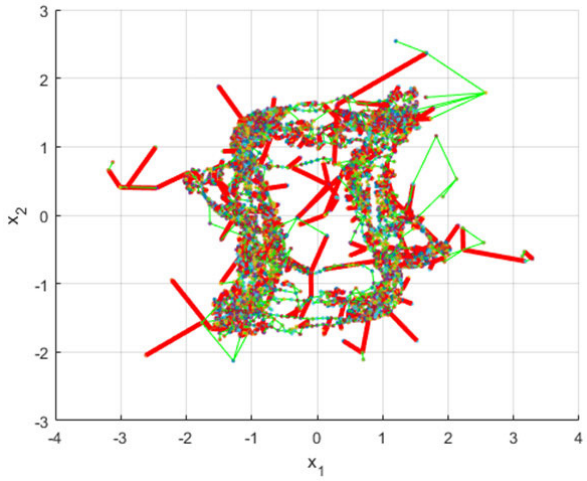

FIGURE 15. Input neurons with connections under 40% load conditions.

are unable to track changes, not allowing its severity to be predicted.

A data topological manifold, the Principal Component Analysis (PCA) [34] has been used to discriminate the clusters better due to healthy and faulty conditions. Fifteen statistical time domain features (see Table 3) were extracted from the current signal by using the affected phase (i.e. phase C) and statistically normalized (z-score) data.

At first, the intrinsic dimensionality was deduced for the affected phase case for the aforementioned data sets (no load, 25% load and 40% load) with the help of Pareto charts (see Figs. 16-18). In all of the three cases, the intrinsic dimensionality has been found to be five, because over 95% of the feature set is explained by using its first five principal components.

Further inspection about the geometry of the feature set has been carried out by using a non-linear DR technique. Based on the conjecture about the intrinsic dimensionality of the feature set via PCA, the CCA (non-linear DR technique) has

TABLE 3. Feature list.

Feature	Definition
Mean	$\bar{x} = \frac{1}{n}\sum_{k=1}^{n}\lvert x_k\rvert$
Maximum Value	$\hat{x} = \max(x)$
Root Mean Square	$RMS = \sqrt{\frac{1}{n}\sum_{k=1}^{n}(x_k)^2}$
Square Root Mean	$SRM = \left(\frac{1}{n}\sum_{k=1}^{n}\sqrt{\lvert x_k\rvert}\right)^2$
Standard Deviation	$\sigma = \sqrt{\frac{1}{n}\sum_{k=1}^{n}(x_k - \bar{x})^2}$
Variance	$\sigma^2 = \frac{1}{n}\sum_{k=1}^{n}(x_k - \bar{x})^2$
RMS Shape Factor	$SF_{RMS} = \frac{RMS}{\frac{1}{n}\sum_{k=1}^{n}\lvert x_k\rvert}$
SRM Shape Factor	$SF_{SRM} = \frac{SRM}{\frac{1}{n}\sum_{k=1}^{n}\lvert x_k\rvert}$
Crest Factor	$CF = \frac{\hat{x}}{RMS}$
Latitude Factor	$LF = \frac{\hat{x}}{SRM}$
Impulse Factor	$IF = \frac{\hat{x}}{\frac{1}{n}\sum_{k=1}^{n}\lvert x_k\rvert}$
Skewness	$S_k = \frac{E(x_k-\bar{x})^3}{\sigma^3}$
Kurtosis	$k = \frac{E(x_k-\bar{x})^4}{\sigma^4}$
Fifth Moment	$M_{5th} = \frac{E(x_k-\bar{x})^5}{\sigma^5}$
Sixth Moment	$M_{6th} = \frac{E(x_k-\bar{x})^6}{\sigma^6}$

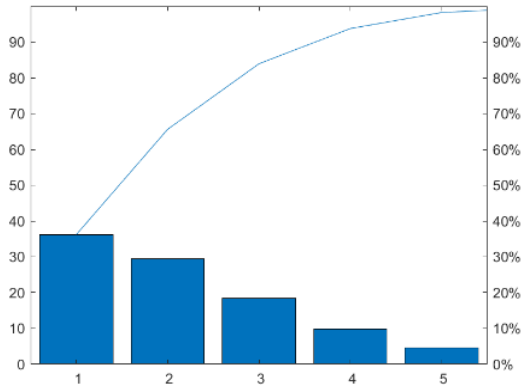

FIGURE 16. Phase C features: Pareto chart under no load conditions.

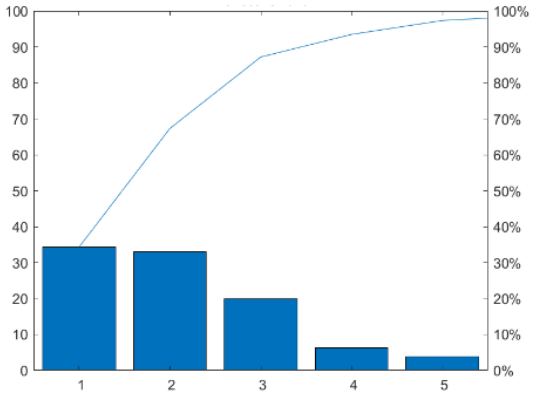

FIGURE 17. Phase C features: Pareto chart under 25% load conditions.

been used to confirm the mapping of the input-output spaces. This mapping can be observed by using the *dy-dx* diagrams. In a nutshell, the CCA neural network has the capability of

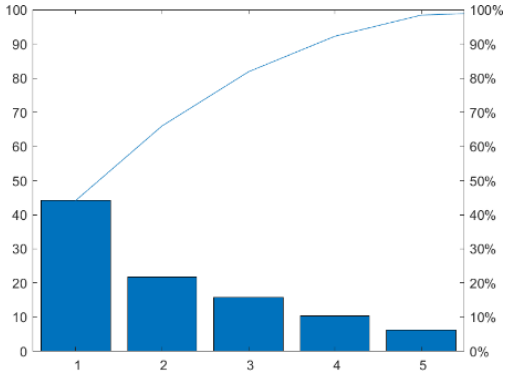

FIGURE 18. Phase C features: Pareto chart under 40% load conditions.

projecting its input into a space of reduced dimension: in doing so, it preserves the data manifold topology by respecting local distances (see [37] for more information). Using this property, the CCA can be used for DR to reduce the number of features without altering the original manifold. This can be validated by using the *dy-dx* diagrams: in these diagrams, the distances of samples in the y-space (*dy*) are plotted against the corresponding distances in the x-space (*dx*). On the one hand, a "*good mapping*" can be obtained when the data points align along the bisector, showing that the distances (*dy* and *dx*) are well preserved. In this case the input dimension can be reduced without losing much information about the data. On the other hand, any deviation of the data cloud from the bisector would represent the non-linear nature of the manifold (i.e. most distances are not respected). In this case, the reduction of the dimension could result in loss of information about the data.

To observe the input-output mapping upon projection of the data in the reduced dimension space of 5, the *dy-dx* plots for 0%, 25% and 40% loading conditions are illustrated in Figs. 19-21. Under 0% loading condition, the data cloud aligns itself onto the bisector (Fig. 19), however, the presence of thick cloud around it represents the noise in data

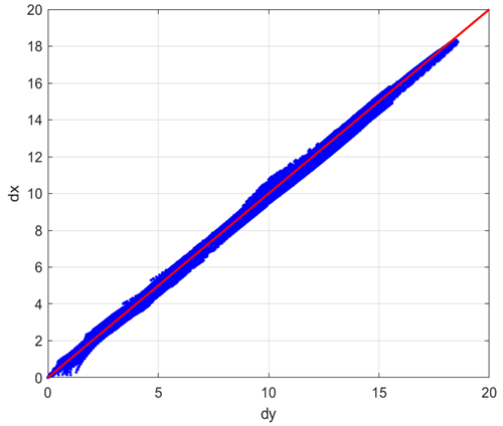

FIGURE 19. Phase C features: CCA dy-dx plot under no load conditions.

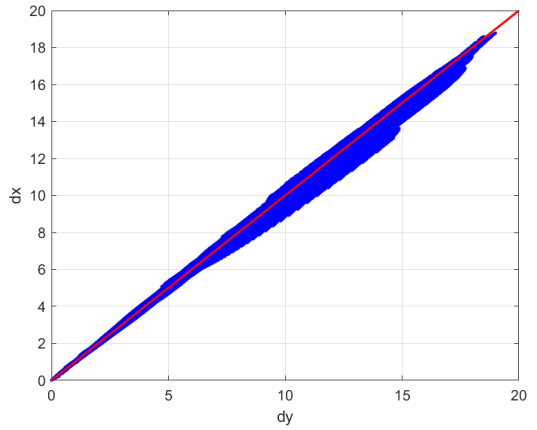

FIGURE 20. Phase C features: CCA dy-dx plot under 25% load conditions.

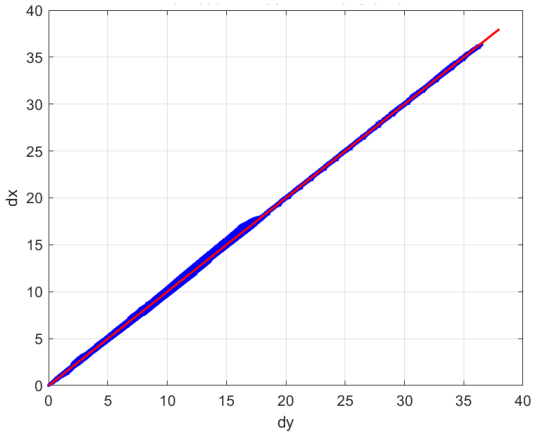

FIGURE 21. Phase C features: CCA dy-dx plot under 40% load conditions.

which is typical for the case of IMs. The point thickness around the origin depicts some element of non-linearity in the dataset with respect to short distances. The manifold is a slightly curved five-dimensional flat (a "*flat*" is a subset of n-dimensional space that is congruent to a Euclidean space of lower dimension).

Fig. 20 obtained with 25% load conditions, resembles Fig. 19, but a large amount of noise is present. Nevertheless, it is apparent that short distances are better preserved in the projection. Middle distances under the bisector can be interpreted as the unfolding of the original dataset. It means that the corresponding manifold is a slightly folded five-dimensional flat.

Finally, the *dy-dx* diagram for 40% load case (see Fig. 21) is quite concentrated around the bisector. Some noise is still present. It seems that the increasing in load condition tends to linearize the manifold, without changing its intrinsic dimensionality.

C. STATOR FAULT EXPERIMENT: DATA AND GCCA QUANTIZATION TOGETHER WITH BRIDGES

Having determined the intrinsic dimensionality in part B above, GCCA has been applied to the three datasets (no load, 25% load and 40% load), by projecting to dimension five. At this aim, input to the GCCA are the temporal features explained in Table 3 for Phase C current. Under this experiment, following are observed:

(a) Transition from healthy to faulty state (fault detection)
(b) Transition between the fault severities

Figures 22-24 show the GCCA quantization in the original 15-dimensional space, using the first three principal components for visualization. Red segments represent the bridges. The healthy cluster is well separated under all loading conditions. Notice the presence of long bridges when there is a transition from one level of fault severity to another. The bridge lengths can be used as an early detector and also as an indicator of the level of fault in case of stator inter-turn faults. This includes abrupt detection of stator faults because lengths observed in the figures represent higher values during transition from healthy to faulty state. In all cases, the healthy cluster (in black color) is well separated from the faulty ones and the transition is always represented by a long bridge, making early fault detection possible on an on-line basis. Under no load condition, separation of the healthy cluster and individual fault severities is well observed. However,

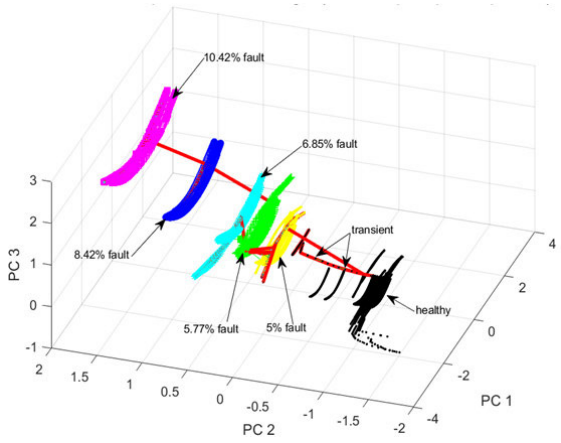

FIGURE 22. Phase C features: GCCA quantization - no load.

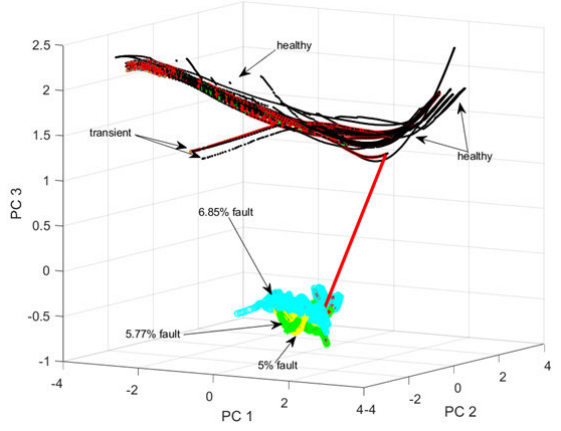

FIGURE 23. Phase C features: GCCA quantization - 25% load.

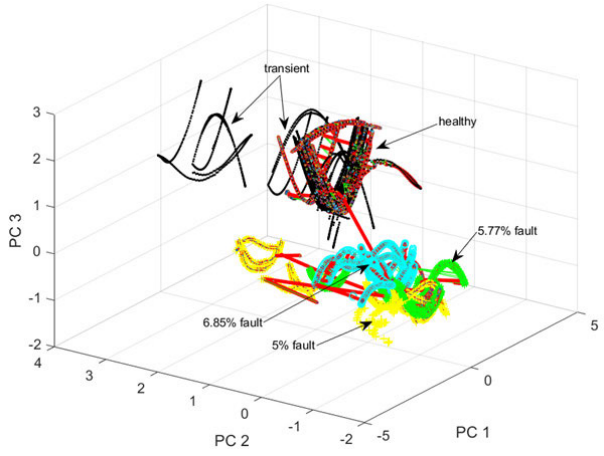

FIGURE 24. Phase C features: GCCA quantization - 40% load.

under loaded conditions, while the healthy cluster (together with its transient cluster) is well separated, the faulty clusters appear to be close by and in some cases, overlapping with other fault severity. This is because of the following reasons: (a) closeness of the severity percentages, (b) additional harmonics introduced due to inverter and external noise, (c) load variation.

V. CONCLUSION

From an industrial point of view, real time tracking of non-stationarities in the data is extremely difficult to achieve, especially when it is time varying. Such is the case in IMs when it comes to stator inter-turn faults.

Due to its reliability and resiliency, GCCA has proved to track abrupt changes successfully in the continuous stream of data. While the linear techniques are mostly used for these types of applications due to its speed and simplicity, non-linear based techniques are computationally expensive and time consuming. The GCCA neural network, unlike them, is the only neural technique that is capable of tracking the non-stationarity in the stream of data generated in the input space and project it in the latent space (a lower dimension space). It is worth mentioning that upon projection to lower dimension space, the GCCA learns the time varying manifold and extracts significant features from the data in the input space.

In case of FD and CM of IMs, this paper shows that GCCA neural network is able to continuously learn the operation of IM (from healthy to faulty cases) under varying load conditions. It is able to clearly isolate the healthy cluster from the faulty ones and tracks the severity of the fault in a very short time. The inception of the fault and its severity can be detected by monitoring the occurrence of bridges and its density estimation, respectively. Thus, damage to the IM can be avoided by stopping its operation.

Due to its capacity of detecting abrupt faults, the GCCA neural network is ideal for systems in which faults are evolving in nature. These systems include: FESS, Fuel Cell and Supercapacitors.

Future work will focus on the classification part by introducing other faulty scenarios as well as on the localization of fault.

REFERENCES

[1] H. Henao, G.-A. Capolino, M. Fernandez-Cabanas, F. Filippetti, C. Bruzzese, E. Strangas, R. Pusca, J. Estima, M. Riera-Guasp, and S. Hedayati-Kia, "Trends in fault diagnosis for electrical machines: A review of diagnostic techniques," *IEEE Ind. Electron. Mag.*, vol. 8, no. 2, pp. 31–42, Jun. 2014.

[2] F. Filippetti, A. Bellini, and G. Capolino, "Condition monitoring and diagnosis of rotor faults in induction machines: State of art and future perspectives," in *Proc. IEEE Workshop Elect. Mach. Design, Control Diagnosis (WEMDCD)*, Mar. 2013, pp. 196–209.

[3] H. A. Toliyat, S. Nandi, S. Choi, and H. Meshgin-Kelk, *Electric Machines: Modeling, Condition Monitoring, and Fault Diagnosis*. Boca Raton, FL, USA: CRC Press, 2012.

[4] A. Accetta, D. Aitchison, G. Cirrincione, M. Cirrincione, M. Pucci, and A. Sferlazza, "Sensorless induction machine drive for fly-wheel generation unit based on a TLS-based non-linear observer," in *Proc. IEEE Symp. Sensorless Control Electr. Drives (SLED)*, Jun. 2016, pp. 1–6.

[5] *IEEE Recommended Practice for the Design of Reliable Industrial and Commercial Power Systems-Redline*, IEEE Standard 493-2007, Revision of IEEE Std 493-1997-Redline, 2007, pp. 1–426.

[6] G. K. Singh and S. Ahmed Saleh Al Kazzaz, "Induction machine drive condition monitoring and diagnostic research—A survey," *Electr. Power Syst. Res.*, vol. 64, no. 2, pp. 145–158, Feb. 2003.

[7] S. Karmakar, S. Chattopadhyay, M. Mitra, and S. Sengupta, *Induction Motor Fault Diagnosis*. Cham, Switzerland: Springer, 2016.

[8] M. El Hachemi Benbouzid, "A review of induction motors signature analysis as a medium for faults detection," *IEEE Trans. Ind. Electron.*, vol. 47, no. 5, pp. 984–993, 2000.

[9] G. B. Kliman, R. A. Koegl, J. Stein, R. D. Endicott, and M. W. Madden, "Noninvasive detection of broken rotor bars in operating induction motors," *IEEE Trans. Energy Convers.*, vol. 3, no. 4, pp. 873–879, 1988, doi: 10.1109/60.9364.

[10] S. Nandi, H. A. Toliyat, and X. Li, "Condition monitoring and fault diagnosis of electrical motors—A review," *IEEE Trans. Energy Convers.*, vol. 20, no. 4, pp. 719–729, Dec. 2005.

[11] A. Siddique, G. S. Yadava, and B. Singh, "A review of stator fault monitoring techniques of induction motors," *IEEE Trans. Energy Convers.*, vol. 20, no. 1, pp. 106–114, Mar. 2005.

[12] Y. Zhongming and W. Bin, "A review on induction motor online fault diagnosis," in *Proc. 3rd Int. Power Electron. Motion Control Conf. (IPEMC)*, vol. 3, 2000, pp. 1353–1358.

[13] R. R. Kumar, G. Cirrincione, M. Cirrincione, A. Tortella, and M. Andriollo, "A topological neural based scheme for classification of faults in induction machines," *IEEE Trans. Ind. Appl.*, early access, Oct. 22, 2020, doi: 10.1109/TIA.2020.3032944.

[14] A. Stavrou, H. G. Sedding, and J. Penman, "Current monitoring for detecting inter-turn short circuits in induction motors," *IEEE Trans. Energy Convers.*, vol. 16, no. 1, pp. 32–37, Mar. 2001.

[15] W. Pietrowski, "Detection of time-varying inter-turn short-circuit in a squirrel cage induction machine by means of generalized regression neural network," *Int. J. Comput. Math. Electr. Electron. Eng.*, vol. 36, no. 1, pp. 289–297, Jan. 2017.

[16] Y. Gritli, L. Zarri, C. Rossi, F. Filippetti, G.-A. Capolino, and D. Casadei, "Advanced diagnosis of electrical faults in wound-rotor induction machines," *IEEE Trans. Ind. Electron.*, vol. 60, no. 9, pp. 4012–4024, Sep. 2013.

[17] S. H. Kia, H. Henao, and G.-A. Capolino, "Diagnosis of broken-bar fault in induction machines using discrete wavelet transform without slip estimation," *IEEE Trans. Ind. Appl.*, vol. 45, no. 4, pp. 1395–1404, Jul. 2009.

[18] M. Riera-Guasp, J. A. Antonino-Daviu, M. Pineda-Sanchez, R. Puche-Panadero, and J. Perez-Cruz, "A general approach for the transient detection of slip-dependent fault components based on the discrete wavelet transform," *IEEE Trans. Ind. Electron.*, vol. 55, no. 12, pp. 4167–4180, Dec. 2008.

[19] A. Stefani, A. Bellini, and F. Filippetti, "Diagnosis of induction Machines' rotor faults in time-varying conditions," *IEEE Trans. Ind. Electron.*, vol. 56, no. 11, pp. 4548–4556, Nov. 2009.

[20] M. Andriollo, R. R. Kumar, A. Tortella, and R. Zavagnin, "FEM based assessment of winding inter-tum fault indicators in line connected induction motors," in *Proc. AEIT Int. Annu. Conf. (AEIT)*, Sep. 2020, pp. 1–6, doi: 10.23919/AEIT50178.2020.9241186.
[21] T. Boukra, A. Lebaroud, and G. Clerc, "Statistical and neural-network approaches for the classification of induction machine faults using the ambiguity plane representation," *IEEE Trans. Ind. Electron.*, vol. 60, no. 9, pp. 4034–4042, Sep. 2013.
[22] M. D. Prieto, G. Cirrincione, A. G. Espinosa, J. A. Ortega, and H. Henao, "Bearing fault detection by a novel condition-monitoring scheme based on statistical-time features and neural networks," *IEEE Trans. Ind. Electron.*, vol. 60, no. 8, pp. 3398–3407, Aug. 2013.
[23] R. R. Kumar, A. Tortella, and M. Andriollo, "Spectral and discriminant analysis based classification of faults in induction machines," in *Proc. AEIT Int. Annu. Conf. (AEIT)*, Sep. 2020, pp. 1–6, doi: 10.23919/AEIT50178.2020.9241115.
[24] R. R. Kumar, G. Cirrincione, M. Cirrincione, M. Andriollo, and A. Tortella, "Accurate fault diagnosis and classification scheme based on non-parametric, statistical-frequency features and neural networks," in *Proc. 13th Int. Conf. Electr. Mach. (ICEM)*, Sep. 2018, pp. 1747–1753, doi: 10.1109/ICELMACH.2018.8507213.
[25] R. R. Kumar, G. Cirrincione, M. Cirrincione, A. Tortella, and M. Andriollo, "Induction machine fault detection and classification using non-parametric, statistical-frequency features and shallow neural networks," *IEEE Trans. Energy Convers.*, early access, Oct. 20, 2020, doi: 10.1109/TEC.2020.3032532.
[26] R. R. Kumar, G. Cirrincione, M. Cirrincione, A. Tortella, and M. Andriollo, "A topological and neural based technique for classification of faults in induction machines," in *Proc. 21st Int. Conf. Electr. Mach. Syst. (ICEMS)*, Oct. 2018, pp. 653–658, doi: 10.23919/ICEMS.2018.8549509.
[27] T. D. Sanger, "Optimal unsupervised learning in a single-layer linear feedforward neural network," *Neural Netw.*, vol. 2, no. 6, pp. 459–473, Jan. 1989.
[28] K. I. Diamantaras and S. Y. Kung, *Principal Component Neural Networks: Theory and Applications*. Hoboken, NJ, USA: Wiley, 1996.
[29] J. Weng, Y. Zhang, and W.-S. Hwang, "Candid covariance-free incremental principal component analysis," *IEEE Trans. Pattern Anal. Mach. Intell.*, vol. 25, no. 8, pp. 1034–1040, Aug. 2003.
[30] X. Qiang, G. Cheng, and Z. Li, "A survey of some classic self-organizing maps with incremental learning," in *Proc. 2nd Int. Conf. Signal Process. Syst.*, vol. 1, Jul. 2010, pp. V1-804–V1-809.
[31] B. Fritzke, "A growing neural gas network learns topologies," in *Proc. Adv. Neural Inf. Process. Syst.*, 1995, pp. 625–632.
[32] T. Martinetz and K. Schulten, "A 'neural-gas' network learns topologies," in *Proc. Int. Conf. Artif. Neural Netw. (ICANN)*, vol. 1, T. Kohonen, K. Makisara, O. Simula, and J. Kangas, Eds. Espoo, Finland: Elsevier, Jun. 1991, pp. 397–402.
[33] G. Cirrincione, J. Herault, and V. Randazzo, "The on-line curvilinear component analysis (onCCA) for real-time data reduction," in *Proc. Int. Joint Conf. Neural Netw. (IJCNN)*, Jul. 2015, pp. 1–8.
[34] G. Cirrincione, V. Randazzo, and E. Pasero, "Growing curvilinear component analysis (GCCA) for dimensionality reduction of nonstationary data," in *Proc. 26th Italian Workshop Neural Netw. (WIRN)*, Vietri sul Mare, Italy: Springer, 2016, pp. 151–160.
[35] R. R. Kumar, V. Randazzo, G. Cirrincione, M. Cirrincione, and E. Pasero, "Analysis of stator faults in induction machines using growing curvilinear component analysis," in *Proc. 20th Int. Conf. Electr. Mach. Syst. (ICEMS)*, Aug. 2017, pp. 1–6.
[36] G. Cirrincione, V. Randazzo, R. R. Kumar, M. Cirrincione, and E. Pasero, "Growing curvilinear component analysis (GCCA) for stator fault detection in induction machines," in *Neural Approaches to Dynamics of Signal Exchanges* (Smart Innovation, Systems and Technologies), vol. 151, A. Esposito, M. Faundez-Zanuy, F. Morabito, and E. Pasero, Eds. Singapore: Springer, 2020, doi: 10.1007/978-981-13-8950-4_22.
[37] P. Demartines and J. Herault, "Curvilinear component analysis: A self-organizing neural network for nonlinear mapping of data sets," *IEEE Trans. Neural Netw.*, vol. 8, no. 1, pp. 148–154, Jan. 1997.
[38] J. Sun, C. Fyfe, and M. Crowe, "Curvilinear component analysis and Bregman divergences," in *Proc. ESANN*, 2010, pp. 81–86.
[39] G. Cirrincione, V. Randazzo, and E. Pasero, "The growing curvilinear component analysis (GCCA) neural network," *Neural Netw.*, vol. 103, pp. 108–117, Jul. 2018.
[40] R. H. White, "Competitive hebbian learning: Algorithm and demonstrations," *Neural Netw.*, vol. 5, no. 2, pp. 261–275, Jan. 1992.
[41] M. Cirrincione, M. Pucci, and G. Vitale, *Power Converters and AC Electrical Drives With Linear Neural Networks*. Boca Raton, FL, USA: CRC Press, 2016.

RAHUL R KUMAR (Student Member, IEEE) received the bachelor's degree in electrical and electronic engineering and the Master of Science in engineering degree from The University of the South Pacific (USP), Suva, Fiji, in 2014 and 2016, respectively. He is currently pursuing the Ph.D. degree with the University of Padova, Padova, Italy. He was awarded a Graduate Assistantship, in 2014, by USP Research Office. Since 2015, he has been a Teaching and Research Assistant with USP. His current research interests include neural networks, system identification, electrical machine fault diagnosis, robotics (armed robots), and data analysis.

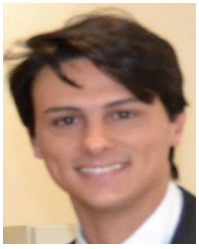

VINCENZO RANDAZZO (Student Member, IEEE) graduated in computer engineering from the Università degli Studi di Palermo. He is currently pursuing the Ph.D. degree with the Politecnico of Turin on the topic offline and online neural networks applied to pattern recognition of big data and IoT (Internet of Things) sensors data. His works have been accepted at IJCNN2015 and WIRN2016, WIRN2017, WIRN2018, SAS2018, ICEMS2017 and IJCNN2018, WIRN2019, and *Neural Networks* journal. His current research interests include neural networks, data analysis, pattern recognition, diagnosis of nonlinear system, electrical drives, and medical and biomedical applications. He is the Former Treasurer of the Politecnico di Torino IEEE Student Branch.

GIANSALVO CIRRINCIONE (Senior Member, IEEE) received the M.S. degree in electrical engineering from the Politecnico di Torino, Italy, in 1991, and the Ph.D. degree (with the congratulations of the jury) from the Laboratoire d'Informatique et Signaux de l'Institut National Polytechnique de Grenoble, Grenoble, France, in 1998. He was a Postdoctoral Scholar with the Department of Signals, Identification, System Theory and Automation (SISTA), Leuven University, Leuven, Belgium, in 1999. Since 2000, he has been an Assistant Professor with the Department of Electrical Engineering, University of Picardie Jules Verne, Amiens, France. He is currently an Adjunct Associate Professor with The University of the South Pacific. His current research interests include neural networks, data analysis, computer vision, brain models, and system identification.

MAURIZIO CIRRINCIONE (Senior Member, IEEE) received the M.S. degree in electrical engineering from the Politecnico di Torino, Italy, in 1991, and the Ph.D. degree in electrical engineering from the University of Palermo, Palermo, Italy, in 1996. From 1996 to 2005, he was a Researcher with the I.S.S.I.A.-C.N.R. Section of Palermo (Institute on Intelligent Systems for Automation), Palermo. Since 2005, he has been a Full Professor of control systems with the University of Technology of Belfort-Montbéliard (UTBM), Belfort, France, where he was a member of the IRTES Laboratory and the Fuel Cell Laboratory (FC Lab). Since April 2014, he has been the Head of the School of Engineering and Physics, The University of the South Pacific, Suva, Fiji. His current research interests include neural networks for modeling and control, system identification, intelligent control, power electronics, power quality, renewable energy systems, control of fuel cell systems, hybrid vehicles, and electrical machines and drives with rotating or linear AC motors.

EROS PASERO (Member, IEEE) is currently a Professor of electronic system engineering with the Department of Electronics and Telecommunications and the Head of the Neuronica Laboratory, Politecnico of Turin. His research interests include artificial neural networks and electronic sensors. Hardware neurons and synapses are studied for neuromorphic approaches; neural software applications are applied to real life proof of concepts. Innovative wired and wireless sensors are also developed for biomedical, environmental and automotive applications. Data coming from sensors are post processed by means of artificial neural networks. He is also the President of SIREN, the Italian Society for Neural Networks, and the General Chairman of WIRN2017, the international Italian workshop for artificial neural networks.

ANDREA TORTELLA (Member, IEEE) received the M.S. degree in electrical engineering and the Ph.D. degree from the University of Padova, Padova, Italy, in 1993 and 1998, respectively. Since 1998, he has been a Researcher with the Department of Electrical Engineering. Since 2011, he was an Associate Professor with the Department of Electrical Engineering. His research interests include design and optimization techniques for linear and rotating permanent magnet machines, adopted in electric propulsion, power generation, and home appliances.

MAURO ANDRIOLLO (Member, IEEE) received the M.S. degree in electrical engineering from the University of Padova, Padova, Italy, in 1985. From 1991 to 1998, he was a Researcher with the Department of Electrical Engineering, University of Padova. From 1998 to 2005, he was an Associate Professor with the Politecnico di Milano, Milan, Italy. Since 2005, he has been an Associate Professor with the University of Padova. His research interests include development of computational methods for electromagnetic analysis and the design and modeling of electrical machines and drives.